

Evaluation of Local 3-D Point Cloud Descriptors in Terms of Suitability for Object Classification

Jens Garstka and Gabriele Peters

*Human-Computer Interaction, Faculty of Mathematics and Computer Science,
University of Hagen, D-58084 Hagen, Germany*

Keywords: Local 3-D Feature Descriptors, Performance Evaluation, Object Classification.

Abstract: This paper investigates existing methods for local 3-D feature description with special regards to their suitability for object classification based on 3-D point cloud data. We choose five approved descriptors, namely Spin Images, Point Feature Histogram, Fast Point Feature Histogram, Signature of Histograms of Orientations, and Unique Shape Context and evaluate them with a commonly used classification pipeline on a large scale 3-D object dataset comprising more than 200000 different point clouds. Of particular interest are the details of the choice of all parameters associated with the classification pipeline. The point clouds are classified by using support vector machines. Fast Point Feature Histogram proves to be the best descriptor for the method of object classification used in this evaluation.

1 INTRODUCTION

Latest advances in image based object recognition, e. g., deep convolutional neural networks may suggest that the problem of object classification is solved. However, it is still possible to list many situations in which deep learning approaches based on image data fail. This happens mainly if the objects are translucent or if they have no or an arbitrary texture, respectively. This is often the case for non-natural human-made objects. Figure 1 illustrates one of these cases.



Figure 1: This patchwork sofa illustrates one of the situations where an image based object recognition or classification is difficult due to arbitrary textures — *image by Dolores Develde, 2012, Creative Commons Attribution 3.0 License.*

To address these problems, it is helpful to regard the 3rd dimension for object classification. It allows to reduce the mentioned problems at least in some cases. The sofa shown in Figure 1, for example, could certainly be recognized using a three-dimensional representation.

A description of 3-D objects can be divided into two broad categories: global and local. Global descriptors define a representation of an object which effectively and concisely describes the entire 3-D object. In most cases, these methods require an a priori segmentation of the scene into object and background and are not suitable for partially visible objects from cluttered scenes. Furthermore, it has to be considered that objects might have different poses or might be deformed. Local descriptors allow robust and efficient recognition approaches that can operate under partial occlusion and are invariant to different poses and deformation.

Beginning with the introduction of Microsoft Kinect in 2010, even research groups with a small budget were enabled to easily generate 3-D data on their own. As a consequence a lot of research regarding local 3-D feature descriptors was done in recent years. This paper investigates five approved local 3-D feature descriptors of 3-D point clouds with a focus on their suitability for object classification. The text is structured as follows. In Section 2, existing evaluations and the evaluated local 3-D feature descriptors are presented. In Section 3 the used classification pipeline is introduced in detail. In Section 4 the five local 3-D feature descriptors are applied and evaluated in context of the classification pipeline. Finally, Section 5 and Section 6 discuss the results and give a short conclusion.

2 RELATED WORK

Subsequently, already published evaluations of local 3-D feature descriptors and the local 3-D feature descriptions considered in this paper are introduced.

2.1 Existing Evaluations

There is a number of publications that deal with evaluations of 3-D feature descriptors in the last five years. A survey and evaluation of local shape descriptors (Heider et al., 2011) divides existing local descriptors into three classes. Focus of the evaluation are 3-D meshes and only local shape descriptors for meshes are examined.

The evaluation of local shape descriptors for 3-D shape retrieval (Tang and Godil, 2012) is similar to the work of (Heider et al., 2011), with the difference that they perform the tests of 6 simple mesh descriptors on the SHREC 2011 Shape Retrieval Contest of Non-rigid 3D Watertight Meshes dataset (Lian et al., 2011).

An evaluation from Alexandre with focus on local 3-D descriptors for object and category recognition (Alexandre, 2012) is the publication that is thematically most similar to our work. The tested algorithms are the same ones as those examined in this paper. However, the pipeline proposed by Alexandre is unsuitable for a larger amount of data.

The evaluation of local 3-D feature descriptors for a classification of surface geometries in point clouds (Arbeiter et al., 2012) investigates how local 3-D feature descriptions can be used to classify primitive local surfaces such as cylinders, edges, or corners in point clouds. Arbeiter et al. compare a small selection of three local 3-D feature descriptors.

The goal of the evaluation of 3-D feature descriptors in the work of (Kim and Hilton, 2013) is a multi-modal registration of 3-D point clouds, meshes, and images. Although the descriptors used in this work are the same as in this paper, conclusions regarding a classification of 3-D point clouds can hardly be derived from their results.

Finally, a survey on 3-D object recognition in cluttered scenes with local surface features (Guo et al., 2014) provides a good overview of the available descriptors and divides them with a taxonomy into different descriptor types. In addition, there is an informal comparison of the performance of each descriptor, which, however, is based on the statements given in each individual publication and not on an own evaluation.

2.2 Local 3-D Feature Descriptors

The goal of local 3-D feature descriptors is the description of particularly “interesting” local areas of a 3-D object. The advantages of local representations consist in their robustness with respect to noise, and their variability concerning object shape and partial occlusions. A wide variety of methods exists (Guo et al., 2014), but not all are suitable for 3-D point clouds, but rather meshes or depth images. The following five local 3-D feature descriptors are suitable for the local description of 3-D point clouds and are evaluated in this paper.

The Spin Image (SI) descriptor (Johnson and Hebert, 1998; Johnson and Hebert, 1999) is arguably the most cited and approved local 3-D descriptor. It is a histogram based method that requires a normal vector as a rotation axis. In a nutshell, all 3-D points of the local environment are collected while the 2-D histogram is rotated around the normal vector.

The Point Feature Histogram (PFH) (Rusu et al., 2008a) is a histogram based approach as well. Rusu et al. compute Darboux frames (Rusu et al., 2008a) for each 3-D point of a local spherical environment. The three angles of each Darboux frame are subdivided into 5 intervals and filled in a histogram with 125 bins.

Since the computational complexity for the determination of Darboux frames at each point within a k -neighborhood is $O(k^2)$, the computation of PFH is relatively slow. For this reason, Rusu et al. proposed a simplified version of PFH named Fast Point Feature Histogram (FPFH) (Rusu et al., 2009). They preserved the basic characteristics of the descriptor, but replaced the computation of the Darboux frame with an approximation of it.

Tombari et al. propose a descriptor called Signatures of Histograms of Orientations (SHOT) (Tombari et al., 2010b; Salti et al., 2014). A spherical neighborhood is divided into several segments. For each segment a histogram is filled with the cosine values of the angles between the z -axis of the local reference frame and the normal vectors of all points that are part of the currently considered segment.

Another local 3-D feature descriptor introduced by Tombari et al. is Unique Shape Context (USC) (Tombari et al., 2010a). It is an extension of the 3-D Shape Context (3DSC) (Frome et al., 2004), which essentially consists of a spherical histogram divided into radial, elevation, and azimuth divisions. Tombari et al. determine a unique local reference frame to ensure that the histogram has unique orientation.



Figure 2: The classification pipeline used for the evaluation of local 3-D feature descriptors. It consists of four main steps: keypoint selection, feature descriptions, a bag-of-words model, and the classification.

3 CLASSIFICATION PIPELINE

At a conceptual level, a 3-D classification pipeline is based on four main steps. These are the keypoint selection (Salti et al., 2011; Dutagaci et al., 2012; Filipe and Alexandre, 2013), the extraction of local feature descriptions (Alexandre, 2012; Guo et al., 2014), a bag-of-words model (Wu and Lin, 2011; Cholewa and Sporysz, 2014), and a machine learning method for the classification task for which support vector machines (Toldo et al., 2010) are widely used. Figure 2 depicts these steps with a conceptual illustration of such a pipeline. The individual steps and their parameters are discussed in detail in the next subsections.

3.1 Point Clouds

The dataset used in the context of this work is the RGB-D Object Dataset (Lai et al., 2011). The dataset contains 51 object classes, e.g., banana, calculator, glue stick, or sponge. Each object class comprises several different objects of the same object class. The object class coffee mug, for example, contains 8 different types of coffee cups. In summary, the datasets contains 300 different objects where each object was captured in different poses. This results in 207841 distinct point clouds. The mean point cloud resolution (*pcr*) of these point clouds is ≈ 0.001295 .

As not only the complete set of object classes, but also a part of it will be used in context of this evaluation, a subset is specified in the following. It consists of 10 randomly selected object classes, namely cap, coffee mug, food bag, greens, hand towel, keyboard, kleenex, notebook, pitcher, and shampoo. These 10 object classes contain approx. 36500 3-D point clouds from 53 distinct objects (cf. Figure 3).



Figure 3: A picture of one object from each of the 10 selected object classes, which are left to right, top to bottom: cap, coffee mug, food bag, greens, hand towel, keyboard, kleenex, notebook, pitcher, and shampoo.

3.2 Keypoint Selection

Keypoints, also referred to as interest points, are points in images or 3-D point clouds that distinctively describe an interesting region. They are supposed to be stable under varying conditions. To ensure that our evaluation results are independent of the choice of a keypoint selection algorithm, two different keypoint selection algorithms are used throughout this paper.

The first method is the keypoint algorithm introduced in context of the Intrinsic Shape Signature (ISS) (Zhong, 2009). According to (Salti et al., 2011) and (Filipe and Alexandre, 2013) the ISS keypoint algorithm yields the best scores in terms of repeatability and is the fastest of the tested algorithms. All relevant parameter values for the Intrinsic Shape Signature keypoint algorithm have been determined in the evaluation of (Salti et al., 2011). Based on their results we use a radius of $6 \cdot pcr$ for our evaluation.

Considering the fact that there are still many current pipelines that rely on sparse sampling (Guo et al., 2014), sparse sampling is used as a second option. The distance of points using sparse sampling varies significantly depending on the approach (Johnson and Hebert, 1998; Frome et al., 2004; Drost et al., 2010; Aldoma et al., 2012b). Thus, we use a radius of $6 \cdot pcr$ for sparse sampling, as well.

3.3 Feature Description

In this subsection we discuss the individual parameters of the five local 3-D feature descriptors (cf. Subsection 2.2) we compare in our evaluation.

3.3.1 Spin Image

There are three main parameters to configure Spin Image (SI): the height, the width, and the radius used for the determination of the normal vector. The height and the width of SI histograms described in (Johnson and Hebert, 1998) is 20×10 . In a later work they propose a size of 15×15 (Johnson and Hebert, 1999), while (Aldoma et al., 2012a) prefer a size of 17×9 . In contrast to Johnson and Hebert, who use meshes in their experiments, Aldoma et al. use point clouds. Furthermore, they use an uneven number of square bins with an edge length equal to the point

cloud resolution to take account of the sparse distribution of point clouds. Therefore, we decided to follow Aldoma et al. and use spin images with a size of $17 \times 9 = 153$ bins for our evaluation. The normal vector will be calculated based on the same radius used to compute the histogram: $9 \cdot pcr$.

3.3.2 Point Feature Histogram

PFH requires two radii, the spherical support area and a radius to approximate the normal vectors of the Darboux frames. The size of the spherical support areas, i. e., the k -neighborhoods, are given by (Rusu et al., 2008a) in meters and centimeters within an interval of $[2.0\text{ cm}, 3.5\text{ cm}]$ for an indoor kitchen scene and $[50\text{ cm}, 150\text{ cm}]$ for an outdoor urban scene. Our test data mainly includes household objects with a size of at most 30 cm . Thus, we can assume that local features can be limited to a size of 5 cm or a k -neighborhood with a radius of 2.5 cm , which fits to the radii that are used by Rusu et al. for the kitchen scene and is approximately equivalent to $19.3 \cdot pcr$.

An indication of the size of the area used for the approximation of the normal vectors is given by (Alexandre, 2012). He proposes a radius of 1 cm which is $\approx 7.7 \cdot pcr$ in our dataset. Therefore, we use a radius of $20 \cdot pcr$ for the spherical support area, and a radius of $8 \cdot pcr$ to approximate the normal vector.

3.3.3 Fast Point Feature Histogram

As the Fast Point Feature Histogram (Rusu et al., 2009) is based on the Point Feature Histogram and follows the same mechanism, we use the same radii as for the Point Feature Histogram.

3.3.4 Signatures of Histograms of Orientations

(Tombari et al., 2010b) recommend histograms with 11 bins and a segmentation of the spherical environment with 8 azimuth divisions, 2 elevation divisions, and 2 radial divisions. Additionally, Tombari et al. specify the size of the support area with $15 \cdot pcr$. We will use all these parameter values for our evaluation, too.

3.3.5 Unique Shape Context

All required parameter values for USC are given by (Tombari et al., 2010a): 10 radial divisions, 14 azimuth divisions, and 14 elevation divisions. The outer radius of the spherical histogram is $20 \cdot pcr$, the inner radius of the spherical histogram is $2 \cdot pcr$, the radius to approximate the normal vector is $20 \cdot pcr$, and the density radius is $2 \cdot pcr$. We use these values in our evaluations as well.

3.4 Bag-of-words

A bag-of-words model is used to count the occurrences of words of a text in a histogram. In the same way a bag-of-words model can be used to count the occurrences of local feature descriptions. In this context it is often called a bag-of-features.

The only parameter required in advance is the number of bins of the histogram. For each bin, a representative local 3-D feature description is required. These descriptions are taken from the centers of each cluster determined by k -means clustering on precomputed local 3-D feature descriptions. The initial centers of the clusters are chosen at random by using a k -means variant named k -means++ (Arthur and Vassilvitskii, 2007). The distance measure used is the Euclidean distance.

Depending on the referred source, the selected number of clusters k differs by orders of magnitude. Toldo et al. use values of k between 20 and 80 (Toldo et al., 2009) and values from 50 to 150 (Toldo et al., 2010), Knopp et al. use 10% of all feature descriptions extracted from a training set as a value of k (Knopp et al., 2010). Madry et al. use between 7 and 300 clusters (Madry et al., 2012; Madry et al., 2013) and Yi et al. use 20% of the average number of features they extracted for each patch of all objects in their training set (Yi et al., 2014). For this reason, 7 different histogram sizes, i. e., 10, 20, 50, 100, 200, 500, and 1000 will be compared in this evaluation.

3.5 Classification

Most of the classification approaches in (Toldo et al., 2009; Toldo et al., 2010; Knopp et al., 2010; Madry et al., 2012; Madry et al., 2013; Seib et al., 2013; Yi et al., 2014) use support vector machines as underlying technique. Only the approach proposed by Yi is based on a different concept using a language model.

Rusu et al. state, that support vector machines have already been used for a classification based on a bag-of-features model for color images with great success (Rusu et al., 2008b; Rusu, 2010). In the referenced works, Rusu et al. test support vector machines, k -nearest neighbor searches, and k -means clustering in different configurations against each other. The best results are achieved using an SVM with a radial basis function (RBF) as kernel. There are some other approaches, e. g., the work presented by (Lai et al., 2011), where in some cases an alternative machine learning approach leads to slightly better results. However, since SVMs are the most widely used classification method in this problem domain, the evaluation presented here will also use SVMs as

binary classifier for each object class. Accordingly, a Gaussian radial basis function is used as kernel.

3.6 Summary

In summary, for a given 3-D point cloud we extract a set of keypoints with ISS and sparse sampling. For each keypoint we compute a local 3-D feature description based on one of the five selected algorithms and determine the nearest representative to count the feature description in the corresponding bin of the bag-of-features histogram. Finally, the bag-of-features histogram is used as input vector for the SVM of each object class and the best matching object class is selected based on the SVM responses.

4 EVALUATION

In this section the evaluation of local 3-D feature descriptors is presented in detail. Initially, the most appropriate keypoint algorithm, the optimal size of a bag-of-features histogram, and the best SVM training parameters are determined. This is done in Subsection 4.1, 4.2, and 4.3. In these subsections, all pipeline parameters are optimized to maximize the correct assignment of an object corresponding to object class C to C . Subsequently, Subsection 4.4 merges these optimizations to an overall classification. Subsection 4.5 examines the computation times required to classify 3-D point clouds this way.

4.1 SVM-parameters

A Gaussian radial basis function

$$K(x_i, x_j) = e^{-\gamma \|x_i - x_j\|^2}, \gamma > 0$$

requires the specification of a single parameter γ which has to be determined depending on the data which is used to train the support vector machine. Additionally, the support vector machine requires a parameter $C > 0$, which is the penalty parameter of the error term, i.e., a multiplier of the distance of misclassified samples to their region.

A Note on SVM Training Histograms:

The following subsections contain small SVM training histograms with the size of 4×4 bins. All these histograms have the same axes and labels. To retain readability, the axes and labels are not included for each histogram. Instead, the labels and axes of all histograms are shown only once in Figure 4. The values of C increase from left to right, while the values of γ increase from top to bottom.

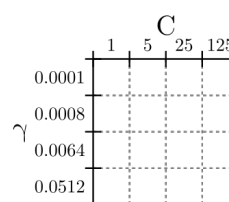


Figure 4: Axes and labels of all SVM training histograms in this paper. C is the penalty parameter for misclassified samples, γ is the parameter of the radial basis function.

4.2 Sparse Sampling vs. ISS

To select the more appropriate keypoint algorithm, the achieved classification rates for both methods, sparse sampling and ISS, are compared.

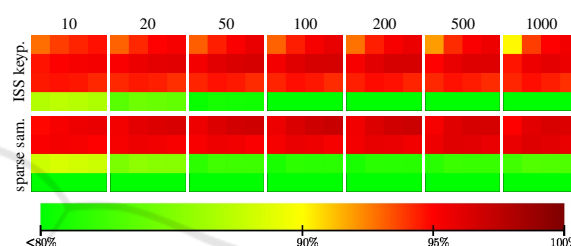


Figure 5: Mean binary classification rates of FPFH – comparison of ISS keypoints and sparse sampling (labels shown in Figure 4). The color scale below the histograms indicates the mean binary classification rates.

Figure 5 illustrates the mean binary classification rates in excerpts for FPFH. Each column represents a bag-of-features size. The upper row illustrates results that can be achieved with keypoints determined by the ISS algorithm, while the lower row contains the results based on sparse sampling. The mean binary classification rates for both methods have nearly the same values shifted by one γ -step. In order to complement the visual interpretation, Table 1 contains the values for ISS with $\gamma = 0.008$ (second row of each ISS histogram) and sparse sampling with $\gamma = 0.001$ (first row of each sparse sampling histogram).

Table 1: Binary classification results for FPFH that can be achieved with ISS keypoints for $\gamma = 0.0008$ and sparse sampling for $\gamma = 0.0001$. (Blue cells: max. value).

BoF	ISS keypoints				sparse sampling			
	$C: 1$	5	25	125	$C: 1$	5	25	125
10	94.66	95.09	95.34	95.47	94.88	95.38	95.68	95.84
20	95.22	95.75	96.04	96.15	95.51	96.06	96.37	96.56
50	95.45	96.12	96.48	96.58	95.67	96.33	96.74	96.90
100	95.46	96.18	96.57	96.65	95.65	96.44	96.92	97.14
200	95.29	96.11	96.56	96.62	95.54	96.33	96.82	97.04
500	94.97	95.91	96.30	96.30	95.32	96.21	96.56	96.66
1000	94.63	95.69	96.02	95.79	95.04	96.13	96.48	96.32

The differences in classification rates between ISS and sparse sampling are always less than 0.5%. This cannot be denoted as significant. For this reason, the number of keypoints should be considered with respect to the computation time. The average number of approx. 355 keypoints per point cloud identified by sparse sampling is more than two and a half times higher, than the average number of approx. 132 keypoints determined by ISS. Accordingly, sparse sampling will not be used due to the larger number of features to be calculated.

4.3 Local 3-D Feature Descriptors

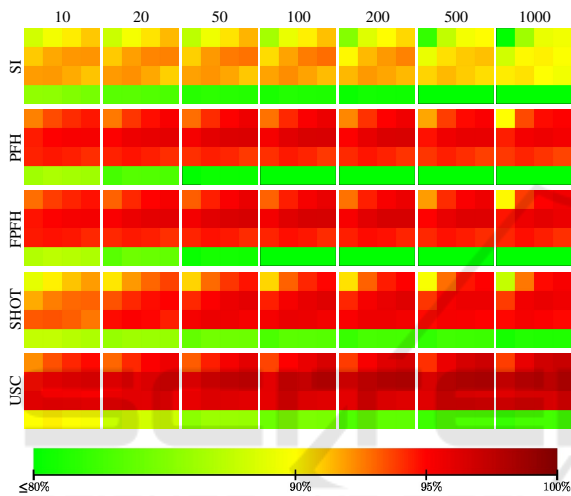


Figure 6: Mean binary classification rates of all evaluated local 3-D feature descriptors (labels shown in Figure 4). The color scale below the histograms indicates the mean binary classification rates.

Figure 6 illustrates the binary classification results for different local 3-D feature descriptors. The low classification results of SI are immediately apparent. Additionally, the darkest shade of red indicating the best classification results can be found for $C = 125$ (right column) and $\gamma = 0.0008$ (second row) of each histogram. Table 2 summarizes the best configuration of parameters for each of the evaluated local 3-D feature descriptors, as well as the corresponding classification rates.

Table 2: Classification rate of the considered descriptors with final set of pipeline parameters. (KP: keypoint algorithm, BoF: size of bag-of-features).

	KP	BoF	C	γ	rate
SI	ISS	50	125	0.008	92.80%
PFH	ISS	100	125	0.008	96.56%
FPFH	ISS	100	125	0.008	96.65%
SHOT	ISS	100	125	0.008	96.27%
USC	ISS	200	125	0.008	97.62%

4.4 Overall Classification Results

The mean binary classification rates shown so far, consider only how well an object corresponding to object class C is correctly assigned to C . In practice, however, it is decisive how often an object corresponding to object class C is incorrectly assigned to another objects class C' . This value is relatively high due to the fact that the shapes of many objects are very similar. Thus, the overall classification rate is by far lagging behind the mean binary classification rate of approx. 96%. In fact, an exact assignment (a point cloud is only assigned to the correct object class and all other SVMs reject the point cloud) can neither be achieved considering all 51 object classes, nor while using the subset of 10 object classes (see Section 3.1).

However, when choosing only that object class where the corresponding SVM returns the highest distance between the input vector (i. e., the bag-of-features histogram) with respect to the separating hyperplane, the classification rates shown in Table 3 can be achieved. Above that, the classification rates that can be achieved for 10 object classes are only slightly lower than those that were achieved by (Alexandre, 2012).

Table 3: Overall classification rates that can be achieved considering the highest distance between the input vector and the separating hyperplane for each SVM.

	51 classes	10 classes
SI	7.4%	23.8%
PFH	6.0%	62.9%
FPFH	9.4%	65.0%
SHOT	3.6%	22.8%
USC	8.5%	59.7%

4.5 Computation Times

The computation times of the five local 3-D feature descriptors may be of particular interest to select one of these algorithms depending on the requirements. Table 4 gives a brief overview of the system used for all computations.

Table 4: System used for evaluation.

Configuration	
CPU	Intel Xeon E5630 @2.53GHz
Memory	12GB DDR3 @1066MHz
OS	Debian 8.0 GNU/Linux 64bit

The average computation times to classify a 3-D point cloud with one of the five local 3-D feature descriptors are shown in Table 5. The values reflect the

computation times that are required for classification. The computation of keypoints, local 3-D feature vectors, and bag-of-feature are not taken into account.

Table 5: Average classification times. The values indicate the time to classify the bag-of-features histogram within each SVM.

	10 classes	all 51 classes
SI	≈ 2.13ms	≈ 10.9ms
PFH	≈ 7.40ms	≈ 37.8ms
FPFH	≈ 2.29ms	≈ 11.7ms
SHOT	≈ 5.85ms	≈ 29.8ms
USC	≈ 3.40ms	≈ 17.3ms

Table 6 shows the mean computation times of a single local 3-D feature description and a factor that enables a quick comparison of the computation times with respect to the fastest algorithm SI.

Table 6: Computation times of 3-D feature description algorithms used within the experiments in ascending order. The last column shows the factor with respect to the fastest algorithm SI.

	Time	Factor
SI	≈ 0.045ms	1
SHOT	≈ 0.28ms	≈ 6
FPFH	≈ 6.69ms	≈ 150
USC	≈ 9.95ms	≈ 220
PFH	≈ 64.51ms	≈ 1430

5 DISCUSSION

Our evaluation of five local 3-D feature descriptors with a focus on 3-D object classification shows, that it is possible to achieve approx. 60% to 65% correct class assignments with PFH, FPFH, and USC (cf. Table 3). The two other algorithms, SI and the SHOT achieve classification rates of only 22% and 23%. In case of SI the mean binary classification rate of 92.80% is considerably lower compared to the other algorithms. The reason for the bad results of SHOT remains unclear. Considering the algorithms with respect to the computation and classification times, SI and SHOT are by far the fastest methods (cf. Table 5 and 6). However, the classification rates of these two algorithms are so low that the two algorithms should not be used in this context. Of the remaining three algorithms FPFH is the fastest and best method, i. e., the method with the highest classification rate at the same time. However, considering the classification results of all local 3-D feature descriptors in context of the full test dataset using all 51 object classes (cf. Table 3) it turns out that a classification of 3-D objects, that are

almost indistinguishable in terms of shape, is in fact not possible. For this reason, the use of local 3-D features can only be seen as a complement to color-based object classification. This is in particular the case when ambiguous textures or bad lighting conditions complicate a color image based method.

6 CONCLUSION

Summarizing, the Fast Point Feature Histogram provides the best results in terms of computation time and classification rate. However, it has to be taken into account that an object classification on the sole basis of 3-D representations only works when the classes are sufficiently different.

REFERENCES

- Aldoma, A., Marton, Z.-C., Tombari, F., Wohlkinger, W., Potthast, C., Zeisl, B., Rusu, R., Gedikli, S., and Vincze, M. (2012a). Tutorial: Point cloud library: Three-dimensional object recognition and 6 dof pose estimation. *Robotics Automation Magazine, IEEE*, 19(3):80–91.
- Aldoma, A., Tombari, F., Rusu, R. B., and Vincze, M. (2012b). Our-cvfh-oriented, unique and repeatable clustered viewpoint feature histogram for object recognition and 6dof pose estimation. In *Pattern Recognition*, pages 113–122. Springer.
- Alexandre, L. A. (2012). 3d descriptors for object and category recognition: a comparative evaluation. In *Workshop on Color-Depth Camera Fusion in Robotics at the IEEE/RSJ International Conference on Intelligent Robots and Systems (IROS), Vilamoura, Portugal*.
- Arbeiter, G., Fuchs, S., Bormann, R., Fischer, J., and Verl, A. (2012). Evaluation of 3d feature descriptors for classification of surface geometries in point clouds. In *2012 IEEE/RSJ International Conference on Intelligent Robots and Systems, IROS 2012, Vilamoura, Algarve, Portugal, October 7-12, 2012*, pages 1644–1650.
- Arthur, D. and Vassilvitskii, S. (2007). k-means++: The advantages of careful seeding. In *Proceedings of the eighteenth annual ACM-SIAM symposium on Discrete algorithms*, pages 1027–1035. Society for Industrial and Applied Mathematics.
- Cholewa, M. and Sporysz, P. (2014). Classification of dynamic sequences of 3d point clouds. In *Artificial Intelligence and Soft Computing*, pages 672–683. Springer.
- Drost, B., Ulrich, M., Navab, N., and Ilic, S. (2010). Model globally, match locally: Efficient and robust 3d object recognition. In *Computer Vision and Pattern Recognition (CVPR), 2010 IEEE Conference on*, pages 998–1005. IEEE.
- Dutagaci, H., Cheung, C. P., and Godil, A. (2012). Evaluation of 3d interest point detection techniques via

- human-generated ground truth. *The Visual Computer*, 28(9):901–917.
- Filipe, S. and Alexandre, L. A. (2013). A comparative evaluation of 3d keypoint detectors. In *9th Conference on Telecommunications, Conftele 2013*, pages 145–148, Castelo Branco, Portugal.
- Frome, A., Huber, D., Kolluri, R., Bulow, T., and Malik, J. (2004). Recognizing objects in range data using regional point descriptors. In *Proceedings of the European Conference on Computer Vision (ECCV)*.
- Guo, Y., Bennamoun, M., Soheli, F., Lu, M., and Wan, J. (2014). 3d object recognition in cluttered scenes with local surface features: A survey. *Pattern Analysis and Machine Intelligence, IEEE Transactions on*, 36(11):2270–2287.
- Heider, P., Pierre-Pierre, A., Li, R., and Grimm, C. (2011). Local shape descriptors, a survey and evaluation. In *Proceedings of the 4th Eurographics conference on 3D Object Retrieval*, pages 49–56. Eurographics Association.
- Johnson, A. and Hebert, M. (1999). Using spin images for efficient object recognition in cluttered 3d scenes. *Pattern Analysis and Machine Intelligence, IEEE Transactions on*, 21(5):433–449.
- Johnson, A. E. and Hebert, M. (1998). Surface matching for object recognition in complex three-dimensional scenes. *Image and Vision Computing*, 16(9):635–651.
- Kim, H. and Hilton, A. (2013). Evaluation of 3d feature descriptors for multi-modal data registration. In *2013 International Conference on 3D Vision, 3DV 2013, Seattle, Washington, USA, June 29 - July 1, 2013*, pages 119–126.
- Knopp, J., Prasad, M., Willems, G., Timofte, R., and Van Gool, L. (2010). Hough transform and 3d surf for robust three dimensional classification. In *Computer Vision–ECCV 2010*, pages 589–602. Springer.
- Lai, K., Bo, L., Ren, X., and Fox, D. (2011). A large-scale hierarchical multi-view rgb-d object dataset. In *Robotics and Automation (ICRA), 2011 IEEE International Conference on*, pages 1817–1824. IEEE.
- Lian, Z., Godil, A., Bustos, B., Daoudi, M., Hermans, J., Kawamura, S., Kurita, Y., Lavoué, G., Van Nguyen, H., Ohbuchi, R., et al. (2011). Shrec’11 track: Shape retrieval on non-rigid 3d watertight meshes. *3DOR*, 11:79–88.
- Madry, M., Afkham, H. M., Ek, C. H., Carlsson, S., and Kragic, D. (2013). Extracting essential local object characteristics for 3d object categorization. In *Intelligent Robots and Systems (IROS), 2013 IEEE/RSJ International Conference on*, pages 2240–2247. IEEE.
- Madry, M., Ek, C. H., Detry, R., Hang, K., and Kragic, D. (2012). Improving generalization for 3d object categorization with global structure histograms. In *Intelligent Robots and Systems (IROS), 2012 IEEE/RSJ International Conference on*, pages 1379–1386. IEEE.
- Rusu, R., Blodow, N., and Beetz, M. (2009). Fast point feature histograms (fpfh) for 3d registration. In *Robotics and Automation, 2009. ICRA ’09. IEEE International Conference on*, pages 3212–3217.
- Rusu, R. B. (2010). Semantic 3d object maps for everyday manipulation in human living environments. *KI-Künstliche Intelligenz*, 24(4):345–348.
- Rusu, R. B., Blodow, N., Marton, Z. C., and Beetz, M. (2008a). Aligning point cloud views using persistent feature histograms. In *Intelligent Robots and Systems, 2008. IROS 2008. IEEE/RSJ International Conference on*, pages 3384–3391. IEEE.
- Rusu, R. B., Marton, Z. C., Blodow, N., and Beetz, M. (2008b). Learning informative point classes for the acquisition of object model maps. In *Control, Automation, Robotics and Vision, 2008. ICARCV 2008. 10th International Conference on*, pages 643–650. IEEE.
- Salti, S., Tombari, F., and Stefano, L. D. (2011). A performance evaluation of 3d keypoint detectors. In *3D Imaging, Modeling, Processing, Visualization and Transmission (3DIMPVT), 2011 International Conference on*, pages 236–243. IEEE.
- Salti, S., Tombari, F., and Stefano, L. D. (2014). Shot: Unique signatures of histograms for surface and texture description. *Computer Vision and Image Understanding*, 125(0):251 – 264.
- Seib, V., Christ-Friedmann, S., Thierfelder, S., and Paulus, D. (2013). Object class and instance recognition on rgb-d data. In *Sixth International Conference on Machine Vision (ICMV 13)*, pages 90670J–90670J. International Society for Optics and Photonics.
- Tang, S. and Godil, A. (2012). An evaluation of local shape descriptors for 3d shape retrieval. *CoRR*, abs/1202.2368.
- Toldo, R., Castellani, U., and Fusiello, A. (2009). A bag of words approach for 3d object categorization. In *Computer Vision/Computer Graphics Collaboration Techniques*, pages 116–127. Springer.
- Toldo, R., Castellani, U., and Fusiello, A. (2010). The bag of words approach for retrieval and categorization of 3d objects. *The Visual Computer*, 26(10):1257–1268.
- Tombari, F., Salti, S., and Di Stefano, L. (2010a). Unique shape context for 3d data description. In *Proceedings of the ACM workshop on 3D object retrieval*, pages 57–62. ACM.
- Tombari, F., Salti, S., and Di Stefano, L. (2010b). Unique signatures of histograms for local surface description. In *Computer Vision–ECCV 2010*, pages 356–369. Springer.
- Wu, C.-C. and Lin, S.-F. (2011). Efficient model detection in point cloud data based on bag of words classification. *Journal of Computational Information Systems*, 7(12):4170–4177.
- Yi, Y., Guang, Y., Hao, Z., Meng-Yin, F., and Mei-ling, W. (2014). Object segmentation and recognition in 3d point cloud with language model. In *Multisensor Fusion and Information Integration for Intelligent Systems (MFI), 2014 International Conference on*, pages 1–6. IEEE.
- Zhong, Y. (2009). Intrinsic shape signatures: A shape descriptor for 3d object recognition. In *Computer Vision Workshops (ICCV Workshops), 2009 IEEE 12th International Conference on*, pages 689–696. IEEE.